

Fluctuation Studies of the (α, p) Reaction on ^{19}F , ^{23}Na , and $^{31}\text{P}^\dagger$

G. G. SEAMAN* AND R. B. LEACHMAN

University of California, Los Alamos Scientific Laboratory, Los Alamos, New Mexico

AND

G. DEARNALEY‡

Atomic Energy Research Establishment, Harwell, England

(Received 13 June 1966; revised manuscript received 13 October 1966)

The (α, p) reaction for many angles between 0° and 175° has been used for fluctuation studies with target nuclei ^{19}F , ^{23}Na , and ^{31}P . Incident energies were 5.2 to 8.0 MeV, 5.9 to 7.9 MeV, and 13.0 to 15.7 MeV, and the measured coherence widths were 50, 35, and 33 keV, respectively. Cross-section peaks were unusually correlated between yields at different angles and between yields to different final states for 5.2- to 5.6-MeV alpha-particle energy on ^{19}F , and so only data above 5.6 MeV were analyzed for fluctuations for this target. The resulting sample sizes in the analyses were then 17, 20, and 27, respectively. Calculations of the effective number of sets of angular-momentum projections damping the fluctuations in the cross sections were used at all angles to determine the additional damping that results from the fraction of direct reactions. For the most forward angles, 0° to 30° , the fraction of direct reactions was generally found to be less than $\frac{1}{2}$ for the ground-state reactions and about 0.6 for the first-excited-state reactions. Even though the data were analyzed for the whole span of energies measured, the modest sample sizes available in these studies resulted in large uncertainties in determining these fractions of direct reactions. Nevertheless, the measured cross sections were in qualitative agreement with both distorted-wave Born-approximation calculations of the direct-reaction cross sections and Hauser-Feshbach calculations of the compound-nucleus cross sections.

I. INTRODUCTION

WHEN nuclei are sufficiently excited that levels of the compound nucleus are widely overlapping, interference effects between incoming and outgoing particles result in fluctuations in the cross section as a function of the incident energy, especially for single exit channels to final states with low spin. Ericson^{1,2} and Brink and Stephen³ have shown that these fluctuations can be formulated in terms of the average width (coherence width) Γ of the compound-nucleus states, the direct-reaction fraction y of the observed cross section, and the effective number N_{eff} of M sets of angular momentum projections that damp the fluctuations as a result of the multiplicity of incoherent emission channels. These sets are $\{s_z, I_z, s_z', I_z'\}$, where s is the projectile spin and I the nuclear spin. In this paper, unprimed quantities are initial conditions and primed are final conditions. Brink *et al.*⁴ have also shown that correlations between the excitation functions obtained at different angles decrease with increasing maximum orbital angular momentum l_{max} imparted by the reaction particles.

Before obtaining these quantities from fluctuation measurements, a verification of the probability distributions of cross section derived by Ericson² and by Brink and Stephen³ was desirable. This was provided by

measurements⁵ of the $^{12}\text{C}(^{12}\text{C}, \alpha)^{20}\text{Ne}$ reaction at energies where direct reactions are negligible. On this basis, many measurements⁶⁻¹⁰ have determined the coherence width Γ for a variety of reactions, all with the necessary condition¹¹ of the instrumental resolution ρ less than the coherence width Γ for direct determinations of the coherence width. An autocorrelation function

$$R(\epsilon) \equiv \delta[(\Delta E - \epsilon)(\Delta E)]^{-1/2} \times \sum_{E_i=E_{\text{min}}}^{E_i=E_{\text{min}}+\Delta E-\epsilon} [x(E_i)-1][x(E_i+\epsilon)-1] \quad (1)$$

⁵ J. Borggreen, B. Elbek, and R. B. Leachman, Kgl. Danske Videnskab. Selskab, Mat. Fys. Medd. **34**, No. 9 (1964); E. Almquist, J. A. Kuehner, D. McPherson, and E. W. Vogt, Phys. Rev. **136**, B84 (1964).

⁶ G. Dearnaley, W. R. Gibbs, R. B. Leachman, and P. C. Rogers, Phys. Rev. **139**, B1170 (1965).

⁷ For earlier references to coherence-width Γ measurements, see Refs. 13, 14, 15, and 16 of the present Ref. 6.

⁸ A. Z. El Behay, M. N. H. Comsan, M. A. Farouk, M. L. Jhingan, and I. I. Zalubovsky, Nuovo Cimento **38**, 1082 (1965); F. Mano, Nucl. Phys. **65**, 419 (1965); H. M. Omar, V. Y. Gontchar, and H. M. S. Baker, Nuovo Cimento **36**, 1388 (1965); J. Ernst, P. von Brentano, and T. Mayer, Phys. Letters **19**, 41 (1965); B. H. Wildenthal, R. W. Krone, and R. W. Prosser, Jr., Phys. Rev. **135**, B680 (1964); F. L. Wilson, University of Kansas Report No. COO-1120-33 (unpublished); J. A. Rawlins, thesis, University of Texas, 1965 (unpublished); I. F. Bubb, J. M. Poate, and R. H. Spear, Nucl. Phys. **65**, 655 (1965); D. von Ehrenstein, L. Meyer-Schützmeister, and R. G. Allas, *ibid.* **79**, 625 (1966); M. Corti, G. M. Marazzan, L. Milazzo Colli, and M. Milazzo, *ibid.* **77**, 625 (1966); W. von Witscher, P. von Brentano, T. Mayer-Kuckuk, and A. Richter, *ibid.* **80**, 394 (1966).

⁹ B. W. Allardyce, P. J. Dallimore, I. Hall, N. W. Tanner, A. Richter, P. von Brentano, and T. Mayer-Kuckuk, Nucl. Phys. **85**, 193 (1966).

¹⁰ L. W. Swenson and K. Izumo, Phys. Letters **19**, 49 (1965).

¹¹ A new method of determining coherence widths Γ for conditions where the experimental resolution ρ is larger ($\rho > \Gamma$), but where both the fraction y of direct reactions and the number N_{eff} of M states can be determined by other means, has been demonstrated by P. Fessenden, W. R. Gibbs, and R. B. Leachman [Phys. Rev. Letters **15**, 796 (1965)].

[†] Work performed under the auspices of the U. S. Atomic Energy Commission.

* Present address: Physics Department, Rutgers, The State University, New Brunswick, New Jersey.

‡ Work done at the Los Alamos Scientific Laboratory while on extended duty from the Atomic Energy Research Establishment.

¹ T. Ericson, Ann. Phys. (N.Y.) **23**, 390 (1963).

² T. Ericson, Phys. Letters **4**, 258 (1963).

³ D. M. Brink and R. O. Stephen, Phys. Letters **5**, 77 (1963).

⁴ D. M. Brink, R. O. Stephen, and N. W. Tanner, Nucl. Phys. **54**, 577 (1964).

between the excitation function and the same excitation function displaced by the energy ϵ is used to determine the coherence width from

$$R(\epsilon) = \frac{R(0)}{1 + \epsilon^2/\Gamma^2}. \quad (2)$$

In Eq. (1), δ is the energy increment of the measurements, which cover the energy span ΔE , and $x = \sigma(E)/\langle\sigma(E)\rangle$ is the normalized cross section $\sigma(E)$ at energy E . In our use, the cross sections σ are always the differential cross sections for emission at angle θ to the incident beam.

The importance of a large sample size in fluctuation analyses has been emphasized by Gibbs.^{6,12,13} To maximize the sample size^{13,14} $n \equiv (\Delta E/\pi\Gamma) + 1$ for the energy region experimentally obtainable and to allow measurement of Γ , target nuclei and incident energies must be chosen that will result in a coherence width that is not greatly larger than the energy spread of the incident particles. In addition, to obtain excitations in the continuum the particles must be of sufficiently high energy that isolated levels are negligible in number. Therefore, in the (α, p) reactions studied here, alpha particles of $E_\alpha = 5.600$ - to 8.035 -MeV, 5.900 - to 7.900 -MeV, and 13.000 - to 15.700 -MeV energy from the Van de Graaff were used for the ^{19}F , ^{23}Na , and ^{31}P targets, respectively. (As indicated by the results considered in Sec. IV, the condition $\Gamma > D$ between state width Γ and spacing D required^{2,3} for fluctuation analyses was generally achieved.) However, the combinations of widths and energy span resulted in sample sizes $n = 17, 20$, and 27 , respectively, smaller than were obtained⁶ for $^{27}\text{Al}(\alpha, p)^{30}\text{Si}$ (but nevertheless larger than in most fluctuation measurements^{7,8,10}), and so the present data for each target are limited to analyses that are statistically reasonable only for larger segments of the energy span measured. In fact, for the present sample sizes, the variations of the coherence width with energy were determined only for segments of $\frac{1}{4}$ or $\frac{1}{6}$ of the energy span.

In the present measurements, three targets of the multiple-alpha-particle-minus-one-proton family of nuclei were used for these fluctuation studies. The previous study⁶ with this type of target gave some evidence of an intermediate resonance. Cross-section fluctuations from this generic group of nuclei might be expected at approximately the same compound-nucleus excitation energy to reveal intermediate resonances¹⁵ of the type discussed by Izumo.^{10,16} In the present

measurements, care was taken to search for these effects.

Determination of the cross sections for compound nucleus σ_{CN} and direct reactions σ_{DI} is an especially interesting result that is difficult to obtain by other means, particularly when the magnitudes of these cross sections are similar. These cross sections are determined by first finding the fraction $y \equiv \sigma_{\text{DI}}/(\sigma_{\text{DI}} + \sigma_{\text{CN}})$ of direct reactions from fluctuations in the measured cross section. The relation

$$R(0) = (1 - y^2)/N_{\text{eff}}, \quad (3)$$

the validity of which has been explored by Gibbs for the $^{27}\text{Al}(\alpha, p)^{30}\text{Si}$ reaction,⁶ is used for this determination of y from the autocorrelation function for any angle, but this requires knowledge of the effective number¹⁷ of M sets of projected angular momentum that, like contributions from direct reactions, also damp¹⁸ the fluctuations. At back angles the fraction y of direct reactions is generally smaller than at forward angles, and so Eq. (3) previously has been used⁶ with the approximation of $y = 0$ for back-angle data to establish the effective number $N_{\text{eff}}^{\text{expt}}$ of M sets from experiment. (In the present study, calculated values of the number of M sets are used instead.)

At the forward angles where direct reactions are expected to be important, the (α, p) reaction experimentally allows a simple method of measuring excitation functions by absorption of the alpha particles. Dearnaley *et al.*⁶ have used such measurements on $^{27}\text{Al}(\alpha, p)^{30}\text{Si}$ with their measured number $N_{\text{eff}}^{\text{expt}}$ of M sets from the supplementary (and thus equivalent for compound-nuclear processes) back angles to determine the fraction of direct reactions at forward angles. This fraction was found to be zero for their lowest incident energies and roughly $\frac{1}{2}$ for their highest energies.

In these cases of ^{19}F , ^{23}Na , and ^{31}P targets, the target spins are, respectively, $\frac{1}{2}$, $\frac{3}{2}$, and $\frac{1}{2}$, and so the limiting number N of M sets

$$N = \frac{1}{2}(2s+1)(2I+1)(2s'+1)(2I'+1) \quad (4)$$

is significantly reduced from the ^{27}Al target case of $I = \frac{5}{2}$. Particularly for the extreme forward and back angles, the low spins of the present targets allow reasonably accurate determinations of the fraction y of direct reactions that lead to the first excited states ($2+$) of the final nuclei. This is because the number N_{eff} of M sets is limited to the small numbers $N = 2, 4$, and 2 for ^{19}F , ^{23}Na , and ^{31}P targets, respectively, as a result of zero projections of orbital angular momenta at 0° and 180° . For these first excited states, the modest fluctuation dampings resulting from these numbers N_{eff} of M sets yield sufficient fluctuations to allow meaningful determinations of the additional fluctuation damping

¹² W. R. Gibbs, Phys. Rev. **139**, B1185 (1965).

¹³ W. R. Gibbs, Los Alamos Scientific Laboratory Report No. LA3266, 1965 (unpublished) (available from Clearing House for Federal Scientific and Technical Information, National Bureau of Standards, U. S. Department of Commerce, Springfield, Virginia).

¹⁴ M. Halbert and M. Bohning, Bull. Am. Phys. Soc. **10**, 120 (1965).

¹⁵ R. B. Leachman, G. Dearnaley, W. R. Gibbs, and G. G. Seaman, Bull. Am. Phys. Soc. **10**, 463 (1965).

¹⁶ K. Izumo, Progr. Theoret. Phys. (Kyoto) **26**, 807 (1961).

¹⁷ J. Bondorf and R. B. Leachman, Kgl. Danske Videnskab. Selskab, Mat. Fys. Medd. **34**, No. 10 (1965).

¹⁸ I. Hall, Phys. Letters **10**, 199 (1964).

from direct reactions. When spurious effects like contaminant peaks, counting statistics, etc., also cause fluctuations, it is particularly important that fluctuations from nuclear effects are large in comparison.

Since the partial cross sections for reactions involving the various M sets of angular momenta projections are generally unequal, the effective number N_{eff} of M sets damping the fluctuations is generally a noninteger number, which is less than the limiting value N . The Hauser-Feshbach¹⁹ approximation [with Eqs. (4) and (5) of Ref. 6] is used to calculate ensemble averages $\bar{\sigma}_\mu$ of these partial cross sections for each of the M sets $\{s_z, I_z, s_z', I_z'\}$. These are combined¹² by

$$N_{\text{eff}}^{\text{a11}} = \left(\sum_{\mu=1}^N \bar{\sigma}_\mu \right)^2 / \sum_{\mu=1}^N (\bar{\sigma}_\mu)^2 \quad (5)$$

to give $N_{\text{eff}}^{\text{a11}}$.

Gibbs²⁰ has now shown that for $N_{\text{eff}}^{\text{a11}}$ actually to be the damping factor in Eq. (3), $N_{\text{eff}}^{\text{a11}}$ is required to be small compared to the effective number Λ of independent reaction amplitudes. Each reaction amplitude is characterized by the set $\{j, l, J, j', l'\}$, where $\mathbf{j} = \mathbf{l} + \mathbf{s}$, l is the orbital angular momentum, and J is the angular momentum of the compound nucleus. Therefore, the number of reaction amplitudes could be very large. (How many of these fill the requirement of being *independent* reaction amplitudes will be considered below.) The number $N_{\text{eff}}^{\text{a11}}$ of $\{s_z, I_z, s_z', I_z'\}$ sets will be small compared to the number of $\{j, l, J, j', l'\}$ sets when orbital angular momenta are large compared to projectile and nuclear spins. For these conditions, the $N_{\text{eff}}^{\text{a11}} \ll \Lambda$ requirement for Eq. (5) is satisfied, and the reaction amplitude for each M set is independent. In this paper, superscripts on calculated N_{eff} terms refer to the number of independent reaction amplitudes, and so the $N_{\text{eff}}^{\text{a11}}$ calculation assumes independent reaction amplitudes for *all* of a very large number of angular momenta combinations in the set $\{j, l, J, j', l'\}$. (Note that $N_{\text{eff}}^{\text{a11}}$ has previously been termed^{6,12} $N_{\text{eff}}^{\text{HF}}$.)

Fluctuation measurements⁶ for the $^{27}\text{Al}(\alpha, p)^{30}\text{Si}$ reaction, for which the number of M sets can be large as a result of $I = \frac{5}{2}$, experimentally showed that the effective number Λ of independent reaction amplitudes was inadequately large compared to this number $N_{\text{eff}}^{\text{a11}}$ of M sets. This was seen by a smaller observed number $N_{\text{eff}}^{\text{expt}}$ of M sets than calculated, $N_{\text{eff}}^{\text{expt}} < N_{\text{eff}}^{\text{a11}}$.

In the following paper, Gibbs²⁰ considers the possibility that the number Λ of independent reaction amplitudes can be approximated by only the effective number of total angular momentum J and parity π values of the compound-nuclear states. This approximation is expected to be valid when the energy span covered is sufficiently small that the population of single-particle states which fracture into the compound-nucleus states does not change significantly. The

Hauser-Feshbach approximation is used again to calculate this effective number of J, π values, and for some of the present cases the effective number of such values is found not to be large compared to the number $N_{\text{eff}}^{\text{a11}}$ of M sets calculated by Eq. (5). For our conditions where the M sets are not independent, the Hauser-Feshbach approximation is used²⁰ to provide a detailed method of calculating the number $N_{\text{eff}}^{J\pi}$ of M sets actually effective in damping fluctuations. An approximate expression for this number

$$N_{\text{eff}}^{J\pi} \approx N_{\text{eff}}^{\text{a11}} [\Lambda / (\Lambda + N_{\text{eff}}^{\text{a11}} - 1)] \quad (6)$$

is also given.²⁰ Our present results provide additional tests of these concepts, but are limited in significance by the uncertainties introduced by the limited sample sizes.

After the number N_{eff} of M sets is determined, Eq. (3) can be used to determine y , which then gives the direct-reaction and compound-nucleus cross sections from the measured cross sections. The present data are analyzed for these cross sections, but the limited sizes of the present data samples cause undesirably large uncertainties in the results. To minimize these uncertainties, only the whole energy span of the data is analyzed. However, any large variation of the fraction of direct reactions with energy as previously observed⁶ then lessens the significance of these single-value determinations.

II. EXPERIMENTAL PROCEDURE

The target chamber, detectors, and recording apparatus have previously been described in detail.⁶ The unusual feature of this arrangement for the forward-angle measurements was the position of the Faraday cup in the center of the chamber so that the alpha-particle beam was stopped in a platinum foil at the back of the Faraday cup, while reaction protons passed through the foil into a 0° detector. All other detectors were covered with gold foils which stopped elastically scattered alpha particles and allowed measurements of only the protons. Back-angle yields and angular distributions were measured in a usual manner.⁶ For the excitation function measurements, the apertures of the detectors were 1.0 cm, which at an average radius of 18 cm corresponds to an angular acceptance of about 3° .

For the $^{31}\text{P}(\alpha, p)$ measurements, a doubly ionized ^4He beam was used to obtain a sufficiently high excitation energy to result in a small coherence width and therefore a reasonably large sample size. The beam was contaminated to varying degrees with deuterons and molecular hydrogen ions, depending upon previous use of the accelerator, which was the Los Alamos single-stage Van de Graaff. These ions have essentially the same charge-to-mass ratio and pass through the analyzing magnet at the same field setting as for $^4\text{He}^{++}$ ions. To measure accurately the $^4\text{He}^{++}$ current alone,

¹⁹ W. Hauser and H. Feshbach, Phys. Rev. **87**, 366 (1952).

²⁰ W. R. Gibbs, following paper, Phys. Rev. **153**, 1206 (1966).

ions elastically scattered from a gold foil placed behind the target were detected in a counter placed at 155° (see Fig. 1). A discriminator level on the pulse-height spectrum allowed only the $^4\text{He}^{++}$ ions to be counted.

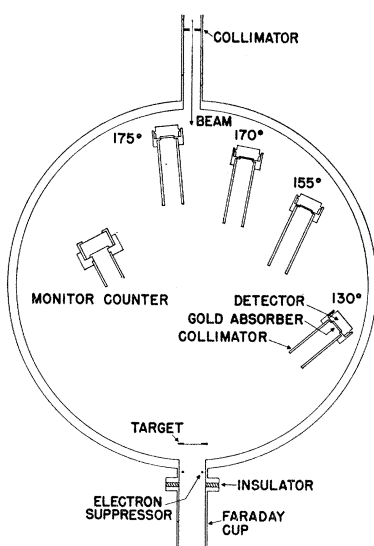
Nickel foil backings of 0.6-mg/cm^2 thickness were used for both the fluorine and sodium targets, which were evaporated deposits of $16.7\text{-}\mu\text{g/cm}^2$ CaF_2 and $22.4\text{-}\mu\text{g/cm}^2$ NaCN . Reaction alpha particles from small contaminations of chlorine in the nickel were energetically resolvable from alpha particles from fluorine, but not from sodium at back angles. Before nickel backings sufficiently free of chlorine contamination were prepared for the data reported here, an evaporated deposit of NaCN on a $25\text{-}\mu\text{g/cm}^2$ carbon backing was attempted. However, the analysis of the data yielded an anomalously large coherence width, indicating that the sodium dissolved into the carbon backing and became a much thicker target. The ^{31}P target used was made in an isotope separator as a deposit of $20\text{ }\mu\text{g/cm}^2$ on a 0.1-mg/cm^2 carbon foil.²¹

The energy loss of alpha particles in the target was combined with the beam resolution to give the total experimental resolution ρ for each target. This was taken to be the width of a rectangular incident-energy resolution. If the true excitation function $\sigma(E)$ can be represented by a parabola for any three neighboring points, then the value of $\sigma(E)$ can be extracted from^{6,22}

$$\sigma(E) = \bar{\sigma}(E) - (\rho^2/24)\bar{\sigma}''(E), \quad (7)$$

where $\bar{\sigma}(E)$ is the experimental excitation function and the double prime indicates the second derivative. The data, shown in Figs. 2 to 4 and used in subsequent analyses, have all been corrected in this manner.

FIG. 1. Experimental arrangement used to measure the excitation functions at forward angles for the case of a $^4\text{He}^{++}$ beam incident on the ^{31}P target. See the text in Sec. II for details.



²¹ We thank A. Katsanos, J. K. Vonach, and J. R. Huizenga of the Argonne National Laboratory for providing this ^{31}P target.

²² Other methods of analysis have been discussed by D. W. Lang, Nucl. Phys. 72, 461 (1965).

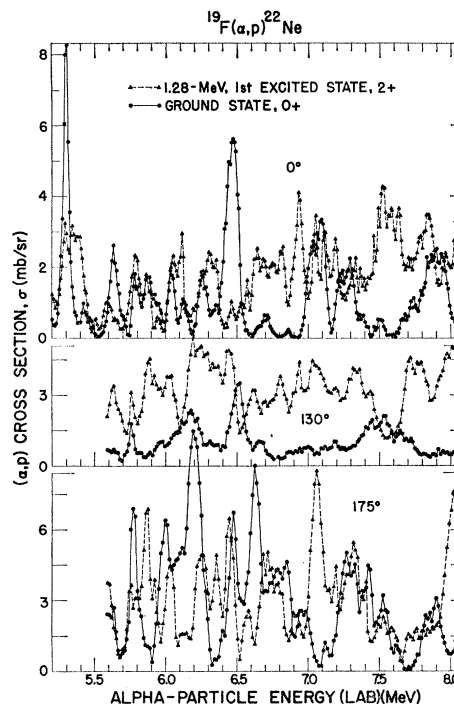


FIG. 2. Excitation functions for three of the eight angles measured for the reaction $^{19}\text{F}(\alpha, p)^{22}\text{Ne}$. Data between 5.2 and 5.6 MeV have apparent cross correlations between ground- and first-excited-state yields and so were not used in fluctuation analyses. The data shown have been corrected (see Sec. II) for the energy spreads of the Van de Graaff beam and introduced by the target thickness. Note different ordinate scales.

III. EXPERIMENTAL RESULTS

A. Excitation Functions

The proton yields to the ground and first-excited states of the residual nucleus for the three targets are given in Figs. 2 to 4 for three representative angles of the angles measured. The target, laboratory angles, incident alpha-particle energy range, and energy increment (δ) used in the measurements follow in order:

^{19}F : $0^\circ, 5^\circ, 15^\circ, 50^\circ$, for 5.200 to 8.030 (0.010) MeV, $130^\circ, 155^\circ, 170^\circ, 175^\circ$ for 5.600 to 8.035 (0.015) MeV;

^{23}Na : $0^\circ, 5^\circ, 15^\circ, 50^\circ$ for 5.910 to 7.8525 (0.0075) MeV; $130^\circ, 155^\circ, 170^\circ, 175^\circ$ for 5.900 to 7.900 (0.020) MeV;

^{31}P : $20^\circ, 50^\circ$ for 13.000 to 15.400 (0.020) MeV, $130^\circ, 155^\circ, 170^\circ, 175^\circ$ for 13.000 to 15.700 (0.020) MeV.

The ^{19}F target for 5.2- to 5.6-MeV alpha particles resulted in unusually large correlation between yields at $0^\circ, 5^\circ, 15^\circ$, and 50° and between ground and first-excited-state yields. However, as shown in Sec. III C, appreciable yield correlation between three angles, $0^\circ, 5^\circ$, and 15° , of these four angles is to be expected. Also,

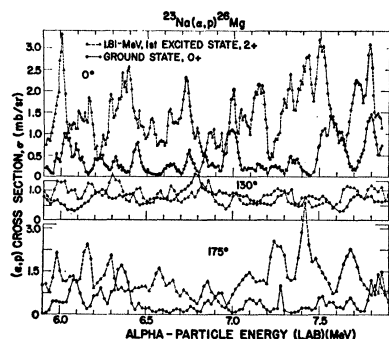


FIG. 3. Excitation functions for three of the eight angles measured for the reaction $^{23}\text{Na}(\alpha, p)^{26}\text{Mg}$. The data shown have been corrected (see Sec. II) for the energy spreads of the Van de Graaff beam and introduced by the target thickness. Note different ordinate scales.

this section shows that state-to-state correlations which include these data result in a poorer agreement with Monte Carlo calculations, but not in unreasonably poor agreement. Furthermore, Sec. IV shows that the measured widths are large compared to the calculated level spacings. These arguments indicate that these correlated peaks are probably not isolated resonances, but nevertheless these 5.2- to 5.6-MeV data were omitted from other calculations. Only ground-state data were resolvable at 20° and 50° for ^{31}P . Changes in the amount of fluctuation with angle and final state can be seen in the excitation functions given in Figs. 2 to 4. At 0° and 175° for the ground state, where $N_{\text{eff}} \approx 1$, the fluctuations in the excitation function are the largest. At 130° and for all angles for the excited state, for which N_{eff} is larger, the excursions from the average value are seen to be reduced.

B. Coherence Widths

The coherence widths Γ are given as a function of energy in Fig. 5. Here, the values from all angles and for

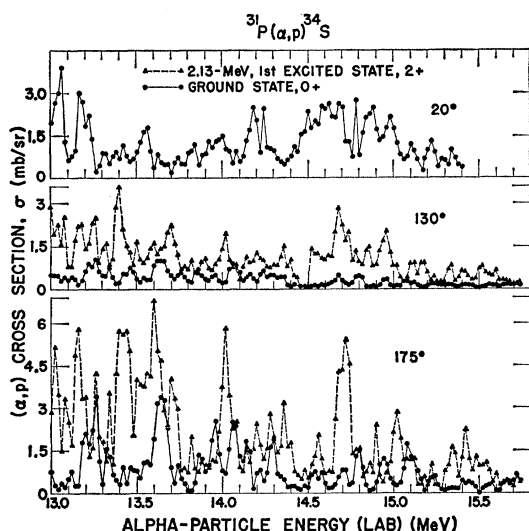


FIG. 4. Excitation functions for three of the six angles measured for the reaction $^{31}\text{P}(\alpha, p)^{34}\text{S}$. The data shown have been corrected (see Sec. II) for the energy spreads of the Van de Graaff beam and introduced by the target thickness.

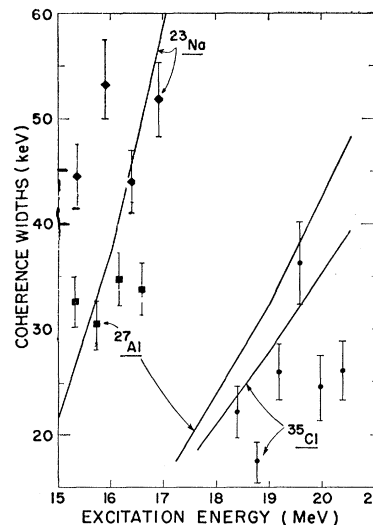


FIG. 5. Coherence widths Γ for the compound nuclei studied. These widths were determined from data for all angles for both ground- and first-excited-state reactions. The widths obtained from the use of the autocorrelation functions of Eq. (2) were corrected for sample size by the method of Refs. 6 and 13. Uncertainties were obtained from the sample sizes n by the method of Ref. 13, but are underestimates of the actual uncertainties since all angles were considered to be uncorrelated. The results of statistical-model calculations, all multiplied by the same constant, are shown by solid curves.

both the ground states and the first excited states have been averaged, and corrections^{6,13} have been made for the sample size n . Widths were calculated from the statistical model⁶ and when these results were multiplied by the same arbitrary constant (to give some agreement with data) the solid curves were obtained. No special effort was made to calculate accurately the transmission coefficients and to select optimum values of statistical-model parameters for these calculated curves, and so the fact that the same arbitrary normalization does not provide good agreement with the different data sets is probably not significant. Although uncertainties are large, the measured widths do not seem to increase as much with energy as calculated. Put *et al.*²³ similarly do not find an observable change of Γ with energy.

The uncertainties^{13,24,25} in the Γ values have been calculated as if the excitation functions at all angles were independent. However, Γ from the excitation function at one angle is independent of Γ from the excitation function at another angle only if the angles are separated by more than the coherence angle. Since this is often not true for our angles (particularly for

²³ L. W. Put, J. D. A. Roeders, and A. von der Woude, in Proceedings of the International Conference on Nuclear Physics, Gatlinburg, 1966 (unpublished).

²⁴ P. J. Dallimore and I. Hall [Nuclear Physics Laboratory, Oxford, Report 175, 1965 (unpublished)] have derived analytical expressions for these uncertainties, but note that they use the number of coherence widths $\Delta E/\Gamma$ as the sample size n .

²⁵ The effects of step size and moving averages on the coherence width Γ have been considered by E. Gadioli, I. Iori, and A. Marini [Nuovo Cimento 39, 996 (1965)], but have not been applied in the present analyses.

0° versus 5° and 170° versus 175°), the number of independent values of Γ is effectively less than the 16 (10 for the ^{31}P case) used for determining the uncertainties. Thus the uncertainties are larger than indicated in Fig. 5. For the whole span of data, the coherence widths were found to be 49.9 ± 2.4 , 35.0 ± 1.6 , and 33.4 ± 1.6 keV for the reactions on ^{19}F , ^{23}Na , and ^{31}P , respectively, with the bias corrections and uncertainties established as above.

C. The Effective Number of M Sets

To calculate the fraction of direct reactions from the autocorrelation values $R(0)$ by Eq. (3), it is first necessary to establish the effective number of M sets damping the fluctuations by incoherent combinations of independent amplitudes. For cases where the fractions of direct reactions are negligible, which sometimes occur at back angles, the experimental value $N_{\text{eff}}^{\text{expt}}$ can be determined by the Gibbs method reported by Dearnaley *et al.*⁶ This involves calculating the autocorrelation function for many sectorings of the data to minimize the effects of any moving average of the cross section.^{6,9,13} However, in the present case, experimental values of $N_{\text{eff}}^{\text{expt}}$ were not useful for three reasons: fractions of direct reactions even at the back angles were appreciable, the number of M sets encountered often exceeded the value 3 allowed by the Gibbs analysis method, and the limited sample sizes resulted in unacceptable uncertainties.

In our cases where the energy span ΔE is not very large compared to the single-particle widths, the number $N_{\text{eff}}^{J\pi}$ calculated by the Gibbs method²⁰ probably provides the most accurate determination of M -set damping. These calculated results are shown in Figs. 6 to 8 along with the number $N_{\text{eff}}^{\text{all}}$ calculated

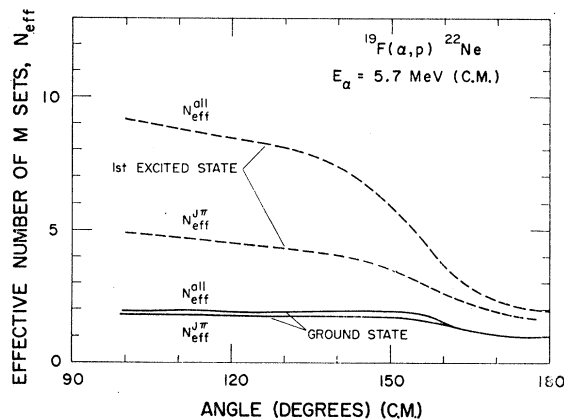


FIG. 6. Comparison of the calculated numbers $N_{\text{eff}}^{\text{all}}$ and $N_{\text{eff}}^{J\pi}$ of M sets for the ^{19}F case. As explained in the text in Sec. III C, the calculated number $N_{\text{eff}}^{\text{all}}$ is based on the assumption that the effective number Λ of independent reaction amplitudes (see Fig. 9) is large compared to the number $N_{\text{eff}}^{\text{all}}$ of M sets. The calculation of $N_{\text{eff}}^{J\pi}$ by the Gibbs method of Ref. 20 assumes that only amplitudes of reactions through states of different J, π are independent.

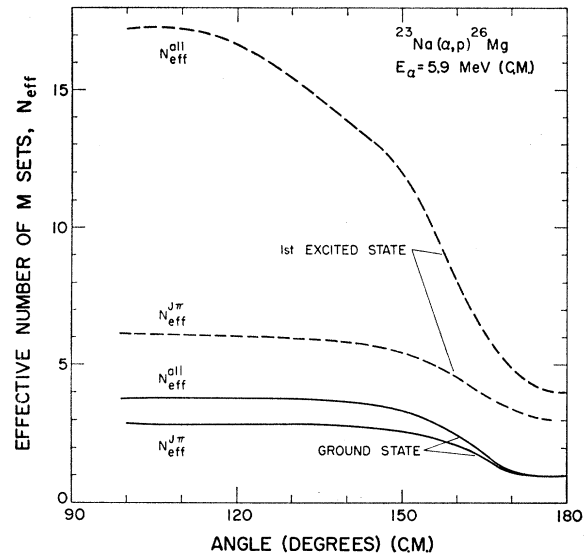


FIG. 7. Comparison of the calculated numbers $N_{\text{eff}}^{\text{all}}$ and $N_{\text{eff}}^{J\pi}$ of M sets for the ^{23}Na case. See the caption to Fig. 6 for other details.

from Eq. (5). These $N_{\text{eff}}^{J\pi}$ values are, of course, lower than the $N_{\text{eff}}^{\text{all}}$ values and agree with the approximation of Eq. (6) when the effective numbers Λ of J, π values calculated by the Gibbs²⁰ method and shown in Fig. 9 are used. The transmission coefficients shown in Figs. 10 to 12 and used in these calculations of both $N_{\text{eff}}^{\text{all}}$ and $N_{\text{eff}}^{J\pi}$ were calculated from the optical-model

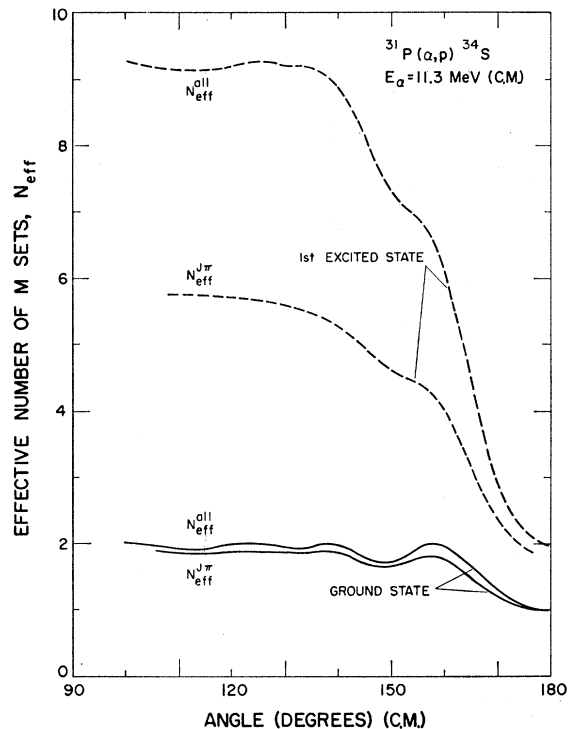


FIG. 8. Comparison of the calculated numbers $N_{\text{eff}}^{\text{all}}$ and $N_{\text{eff}}^{J\pi}$ of M sets for the ^{31}P case. See the caption to Fig. 6 for other details.

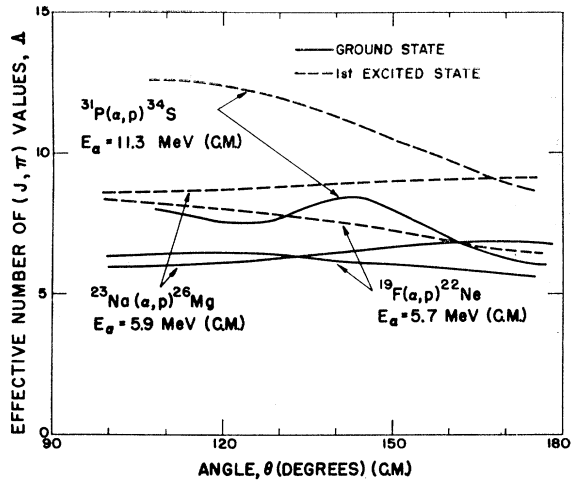


FIG. 9. The effective number A of total angular momentum J and parity π values for compound nuclei in the (α, p) reactions on ^{19}F , ^{23}Na , and ^{31}P to the ground and first excited states of the final nuclei. The Gibbs calculation of Ref. 20 is used to determine these values. Section III C of the text contains a brief discussion of this calculation.

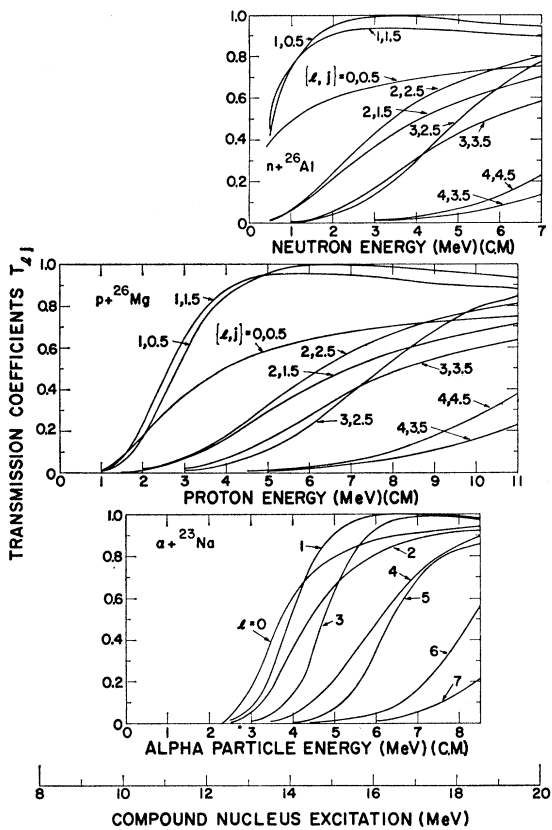


FIG. 10. Transmission coefficients T_{lj}^{γ} calculated by the optical model for various exit channels γ for the compound nucleus ^{23}Na formed by alpha particles incident upon ^{19}F . The orbital angular momenta l and the particle spin s combine to form j . Abscissas are displaced to the common excitation energy of the compound system. Optical-model parameters were from Ref. 26 for alpha particles and from Ref. 27 for protons and neutrons.

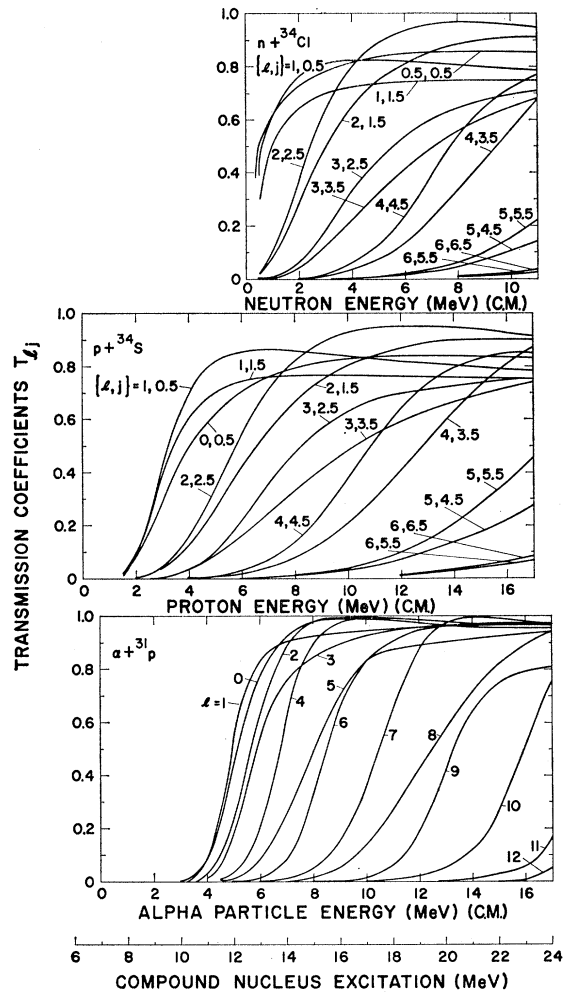


FIG. 11. Transmission coefficients T_{lj}^{γ} calculated by the optical model for various exit channels γ for the compound nucleus ^{27}Al formed by alpha particles incident upon ^{23}Na . See the caption to Fig. 10 for other details.

potentials of Huizenga and Igo²⁶ for alpha particles and of Rosen *et al.*²⁷ for protons and neutrons. In these calculations, a number of exit channels²⁸ totaling 34 for ^{19}F and 35 for ^{23}Na were used as required for alpha-particle, neutron, and proton emission. For the ^{31}P target, where larger excitations are involved, every third level for exit channels was used up to a total of 40 exit channels.

²⁶ J. R. Huizenga and G. Igo, Nucl. Phys. **29**, 462 (1962) and Argonne National Laboratory Report No. ANL6373, 1961 (unpublished).

²⁷ L. Rosen, J. G. Beery, A. S. Goldhaber, and E. H. Auerbach, Ann. Phys. (N.Y.) **34**, 96 (1965).

²⁸ Experimentally observed states given by P. M. Endt and C. van der Luen [Nucl. Phys. **34**, 1 (1962)] and, for lighter elements, by T. Lauritsen and F. Ajzenberg-Selove [Nuclear Data Sheets, compiled by K. Way *et al.* (Printing and Publishing Office, 1962, National Academy of Sciences—National Research Council, Washington, D. C.)] were used. Where spins, parities, or energies of the levels were not known, assignments were made that agreed with distributions specified by the parameters of A. Gilbert and A. G. W. Cameron [Can. J. Phys. **43**, 1446 (1965)].

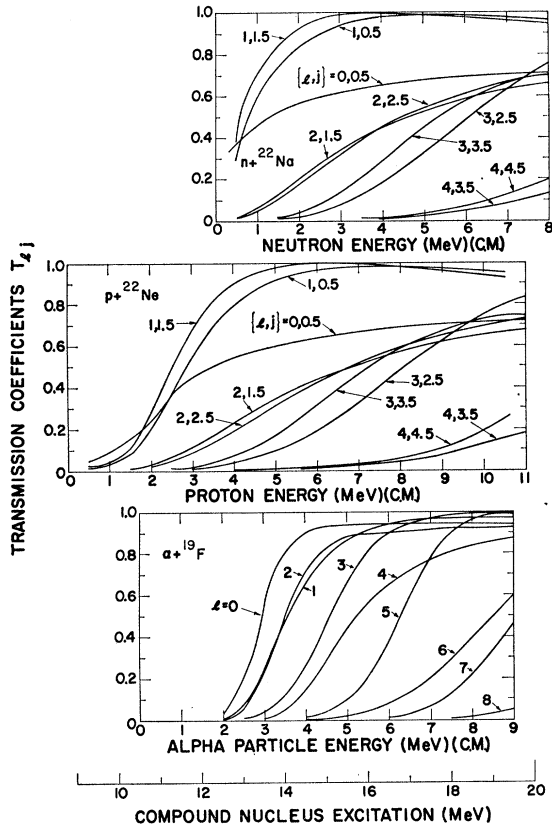


FIG. 12. Transmission coefficients $T_{l,j}$ calculated by the optical model for various exit channels γ for the compound nucleus ^{35}Cl formed by alpha particles incident upon ^{31}P . See the caption to Fig. 10 for other details.

D. Direct and Compound-Nucleus Reactions

The measured autocorrelation functions R and the calculated numbers $N_{\text{eff}}^{J\pi}$ of M sets (Figs. 6 to 8 for the indicated angles and the supplementary angles) are now used with Eq. (3) to determine the fraction γ of direct reactions for all angles measured. Here, R values were determined from the whole span of data, and so any moving average effects have not been eliminated. The fractions γ of direct reactions thus obtained are shown in Fig. 13. The large uncertainties in γ are from the uncertainties in R that result from the moderately small sample sizes^{6,13} and from the fact that the γ values are not close to unity. These uncertainties do not include any uncertainty in the method of calculating N_{eff} .

Since the average cross sections $\langle\sigma\rangle$ are readily obtained from the measurements, the compound-nucleus cross sections $\langle\sigma_{\text{CN}}\rangle$ and direct-reaction cross sections $\langle\sigma_{\text{DI}}\rangle$ can be obtained from the γ results in Fig. 13 through the relation $\langle\sigma\rangle = \langle\sigma_{\text{CN}}\rangle + \langle\sigma_{\text{DI}}\rangle$. These results are shown in Figs. 14 to 16. Shown in comparison with these results are calculated values of the direct-reaction and compound-nucleus cross sections. The direct-reaction cross sections were calculated²⁹ by the

²⁹ We thank W. R. Gibbs for these calculations.

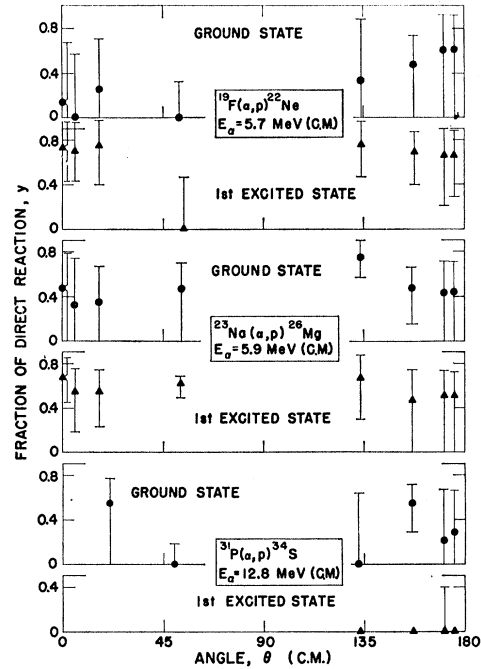


FIG. 13. Fractions γ of direct reactions at measured angles as determined from fluctuation analyses. Uncertainties were obtained from the sample sizes by the method of Ref. 13. The γ values were determined from Eq. (3) with the use of the calculated $N_{\text{eff}}^{J\pi}$ values of Figs. 6 to 8 and R values determined from the whole span of energy. The R values were corrected for finite sample size, but not for any moving average effect.

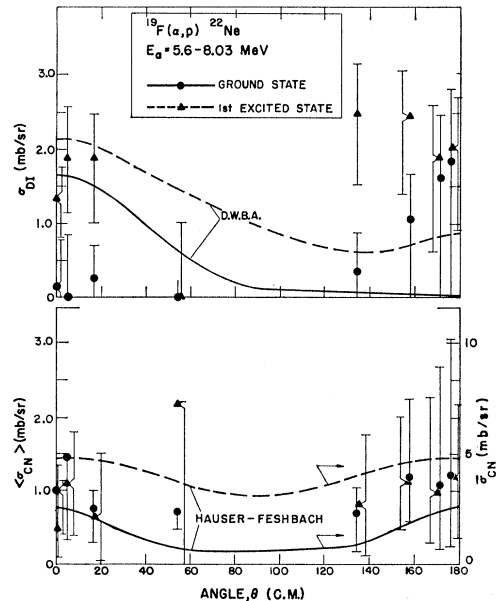


FIG. 14. The direct-reaction cross section σ_{DI} and compound-nucleus cross section σ_{CN} for $^{19}\text{F}(\alpha, p)^{22}\text{Ne}$. The experimental values shown as points were determined by the analysis described in Secs. III D and IV. The distorted-wave Born-approximation calculations were made with $l=0$ and $l=2$ angular-momentum transfer of a triton for the ground-state and first-excited-state reactions, respectively. These calculated σ_{DI} curves have the same $\frac{2}{3}$ factor of normalization in Figs. 14 to 16. The Hauser-Feshbach calculation of σ_{CN} is described in Secs. III C and IV.

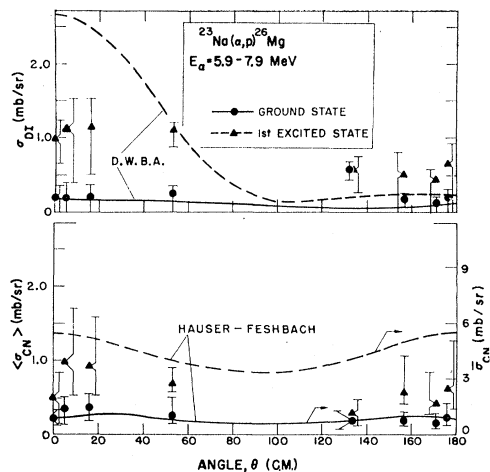


FIG. 15. The direct-reaction and compound-nucleus cross sections for $^{23}\text{Na}(\alpha, p)^{26}\text{Mg}$. The distorted-wave Born-approximation calculations were made with $l=2$ and $l=0$ angular-momentum transfer for the ground- and first-excited-state reactions, respectively. See the caption to Fig. 14 for other details.

distorted-wave Born-approximation method, in which transfer of a triton was used. Parameters used in the calculations are given in Table I. The calculated results were all normalized by a factor of $\frac{2}{3}$ for presentation in Figs. 14 to 16. The compound-nucleus cross sections $\bar{\sigma}_{\text{CN}}$ were calculated by the Hauser-Feshbach method with the parameters given in the previous section. [The calculated results for $^{31}\text{P}(\alpha, p)^{34}\text{S}$ were reduced by a factor of 3 to compensate for the use of only every third level in the calculation.]

Comparison between these measured and calculated results is made in Sec. IV.

E. Intermediate Resonance Search

At the compound-nucleus excitation energies E^* of 16.65 to 16.91 MeV in the $^{27}\text{Al}(\alpha, p)$ reaction, the autocorrelation function $R(0)$ was found to be small at all angles.⁶ This represents a damped region in the cross-section fluctuations of about 0.3-MeV energy span and was interpreted⁶ as evidence for intermediate resonances.^{10,30,31} Similar regions were found¹⁵ in ^{19}F and ^{23}Na excitation functions for forward angles at about $E^* \approx 16.2$ -MeV compound-nucleus excitation energies. However, further data taken at back angles for ^{19}F and ^{23}Na gave little evidence of the same damped region. Some of these data are shown in Figs. 2 and 4. Thus no damped region at about the same excitation energy in all these generically related nuclei is seen.

Statistically, a region of small fluctuation might be expected³² occasionally for some target nucleus to some particular exit channel. The absence of a similar region for the target nuclei in the present study argues for this

statistical explanation for the $^{27}\text{Al}(\alpha, p)^{30}\text{Si}$ first-excited-state result rather than an intermediate-structure explanation.

Another test was made to see if these $E^* \approx 16.2$ -MeV excitation energy regions of damping for some angles in the present study would possibly be regions of intermediate structure characterized by one angular momentum state. The angular distributions shown in Figs. 17 and 18 show no evidence of such single-state characteristics for this energy region, but show for all energies the complicated distributions expected from overlapping compound-nucleus levels of different angular momenta.

F. Cross Correlation Functions

Cross correlation functions $C_{12}(\epsilon)$ have been calculated from the expression

$$C_{12}(\epsilon) = \delta[\Delta E(\Delta E - \epsilon)R_1(0)R_2(0)]^{-1/2}$$

$$\times \sum_{E_i=E_{\min}}^{E_i=E_{\min}+\Delta E-\epsilon} [x_1(E_i)-1][x_2(E_i+\epsilon)-1], \quad (8)$$

where $R_1(0)$ and $R_2(0)$ are the autocorrelation functions for excitation functions 1 and 2.

The cross correlations have been calculated for each state between different angles to determine the coherence angle. As shown in Fig. 19 the coherence angle decreases with the increasing angular momentum transfer from the ^{19}F , ^{23}Na , to ^{31}P cases as expected from the analytical expression for coherence angle.⁴

Cross correlations between states have been made to determine the importance of possibly isolated resonances. These are shown in Fig. 20. The solid curves are Monte Carlo calculations²⁹ for n independent cross-section distributions, each with a four-degrees-of-

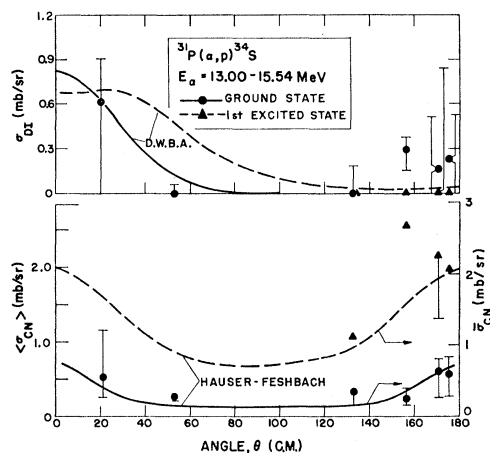


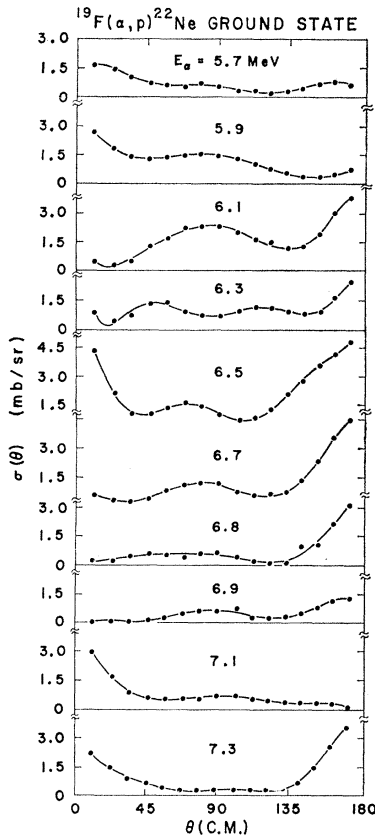
FIG. 16. The direct-reaction and compound-nucleus cross sections for $^{31}\text{P}(\alpha, p)^{34}\text{S}$. The distorted-wave Born-approximation calculations were made with $l=0$ and $l=2$ angular-momentum transfer for the ground- and first-excited-state reactions, respectively. See the caption to Fig. 14 for other details.

³⁰ K. Izumo, Progr. Theoret. Phys. (Kyoto) 26, 807 (1961).

³¹ B. Bloch and H. Feshbach, Ann. Phys. (N.Y.) 23, 47 (1963).

³² P. P. Singh, P. Hoffman-Pinther, and D. W. Lang, Phys. Letters 23, 255 (1966).

FIG. 17. Angular distributions for the $^{19}\text{F}(\alpha, p)^{22}\text{Ne}$ reaction to the ground state. Curves are least-squares fits to the data with Legendre polynomial sums to seventh order. Section III E of the text interprets the complex angular distributions to indicate that any intermediate-resonance effects are not important. These angular distributions were measured with a target in the center of the chamber and with the four counters at 21° spacings on a single movable arm. The counters had a 1.0-cm-diam aperture and were at a radius of 10 cm.



freedom χ^2 distribution ($N=2$). Approximately the same number n of distributions were used as were obtained in the cross-section data. For the ^{19}F target, the histogram for the range 5.20 to 8.03 MeV for the four forward angles measured at these lower energies has been included as dotted lines. These results show

TABLE I. Parameters used in distorted-wave Born-approximation calculations of direct-reaction cross sections for transfer of a triton in (α, p) reactions on ^{19}F , ^{23}Na , and ^{31}P . Potential-well depth is designated by V , radius by R , and diffuseness by a . Subscripts denote: α for alpha particle, p for proton, t for triton, Re for real part, and Im for imaginary part.

Target State	^{19}F		^{23}Na		^{31}P	
	Gnd	First	Gnd	First	Gnd	First
Q (MeV)	1.700	0.421	1.826	0.016	0.631	-1.500
l value	0	2	2	0	0	2
E_α (c.m.) (MeV)	5.64		5.89		12.80	
$V_{\text{Re}, \alpha}$ (MeV)	-50.0		-50.0		-50.0	
$V_{\text{Im}, \alpha}$ (MeV)	-5.3		-5.3		-5.3	
R_α (F)	4.89		5.16		5.44	
a_α (F)	0.58		0.58		0.58	
$V_{\text{Re}, p}$ (MeV)	-51.0		-51.9		-57.8	
$V_{\text{Im}, p}$ (MeV)	-5.5		-5.5		-7.5	
R_p (F)	3.34		3.56		4.05	
a_p (F)	0.65		0.65		0.65	
R_t (F)	3.34		3.56		4.05	

that the ^{19}F case where the 5.2- to 5.6-MeV data were included (data that were omitted in other analyses) the cross correlations are somewhat greater than expected by chance. Comparison of the observed cross correlations with the calculated cross correlations for the ^{23}Na case in Fig. 20 shows a predominance of positive values that statistically are barely significant. However, observation of the excitation functions gives no indication of peaks correlated between the ground- and first-excited-state yields. Thus, in the analyses made in this paper we consider the effects of any isolated levels always to be unimportant.

IV. DISCUSSION

For the Ericson² and Brink and Stephen³ type of analysis to be valid, the width of the compound-nuclear levels must exceed the spacing, $\Gamma/D > 1$, even at the lowest excitation energies where this ratio is expected to be lowest. The measured widths are shown in Fig. 5. The spacings D are calculated from Gilbert and Cameron.²⁸ Then for the lowest energies we find: $D=1.6$ keV and $\Gamma/D=27$ for the fluorine target; $D=1.2$ keV and $\Gamma/D=28$ for the sodium target; and $D=0.11$ keV and $\Gamma/D=201$ for the phosphorus target. Although level spacings calculated by the statistical model at these large excitation energies are uncertain, these large width-to-spacing ratios give some assurance that the fluctuation analyses are valid. The agreements between the observed and expected cross correlations in Fig. 20 give added assurance.

One of the main purposes of the present investigation was to determine the direct-reaction cross sections for various target masses. The $(1-\gamma^2)$ term in Eq. (3) results in sensitive determinations of the fraction γ of direct reactions only when γ approaches unity. Just as

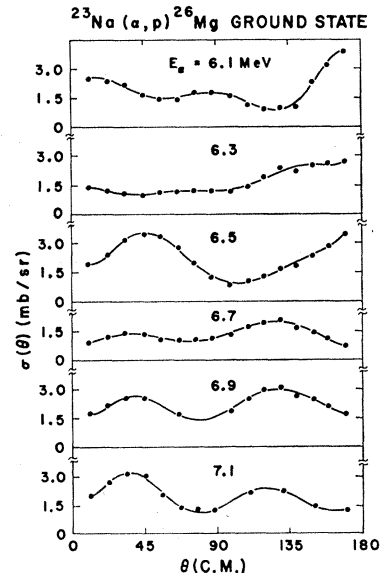


FIG. 18. Angular distributions for the $^{23}\text{Na}(\alpha, p)^{26}\text{Mg}$ reaction to the ground state. See the caption to Fig. 17 for other details.

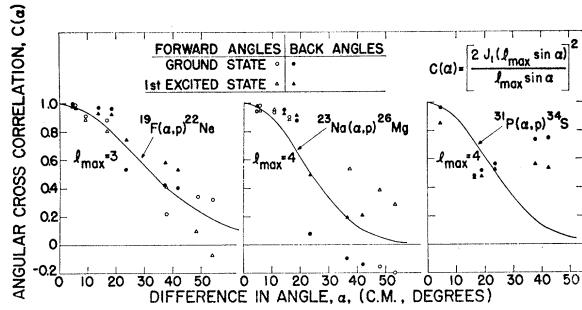


FIG. 19. Angular-cross-correlation functions $C_0(\alpha)$ and $C_1(\alpha)$ for ground-state and first-excited-state reactions, respectively, for angular differences α between data. Results for ^{19}F , ^{23}Na , and ^{31}P are shown. The cross correlations were calculated from Eq. (8).

in the case of the previously studied $^{27}\text{Al}(\alpha, p)^{30}\text{Si}$ reaction,⁶ γ was generally found to be about one-half or less, and so the determinations have large uncertainties for the limited finite sample sizes n available in the fluctuation analyses.

The direct-reaction cross sections σ_{DI} and compound-nucleus cross sections $\langle\sigma_{\text{CN}}\rangle$ found from the data and shown in Figs. 14 to 16 have two other limitations that should be considered when these results are compared with the Hauser-Feshbach calculations $\bar{\sigma}_{\text{CN}}$ and the distorted-wave Born-approximation calculations, respectively, in these figures. One is that the results are from roughly 2-MeV spans of incident energy, over which the fraction of direct reactions could be expected to change significantly. This was found at these energies for the $^{27}\text{Al}(p, \alpha)^{31}\text{Si}$ reaction.⁶

The other limitation is that the calculated number $N_{\text{eff}}^{J\pi}$ of M sets used in Eq. (3) for the analyses is possibly an underestimate of the number N_{eff} actually effective. The number $N_{\text{eff}}^{J\pi}$ used is calculated from the effective number of J, π values of compound-nuclear levels that all stem from the same single-particle states. However, the effective number N_{eff} of M sets would be larger than $N_{\text{eff}}^{J\pi}$, but less than $N_{\text{eff}}^{\text{all}}$, if the single-particle widths are less than the approximately 2-MeV energy span covered in the measurements. Thus, particularly for the first-excited-state reactions where $N_{\text{eff}}^{J\pi}$ and $N_{\text{eff}}^{\text{all}}$ differ greatly at angles away from 0° and 180° as seen by Figs. 6 to 8, the fractions of direct reactions γ determined from calculated values of $N_{\text{eff}}^{J\pi}$ possibly result from the use of an underestimate of N_{eff} and so are possibly somewhat large. Consequently, in Figs. 14 to 16, the σ_{DI} values for these cases can err in being large, and the $\langle\sigma_{\text{CN}}\rangle$ values can have a corresponding error in being small.

These errors are, however, unlikely for the ground-state reactions. Here, the number $N_{\text{eff}}^{\text{all}}$ of M sets is small compared to the effective number Λ of J, π values in the compound nucleus, and so $N_{\text{eff}}^{J\pi}$ can be seen by Eq. (6) to approach $N_{\text{eff}}^{\text{all}}$. The calculated results in Figs. 6 to 8 confirm this, particularly for the low-spin cases of ^{19}F and ^{31}P .

We now consider the compound-nucleus cross section $\langle\sigma_{\text{CN}}\rangle$ measurements in Figs. 14 to 16. In general, these $\langle\sigma_{\text{CN}}\rangle$ results are symmetrical about 90° with a smaller cross section near 90° , as expected from angular momentum and nuclear moment-of-inertia considerations.³³ These properties are, of course, obtained from the cross sections $\bar{\sigma}_{\text{CN}}$ obtained from the Hauser-Feshbach calculations. The fact that larger $\bar{\sigma}_{\text{CN}}$ values were calculated than the measured $\langle\sigma_{\text{CN}}\rangle$ values is largely to be attributed to the omission of competing exit channels to levels that have not been reported.²⁸ To a lesser extent, the calculated $\bar{\sigma}_{\text{CN}}$ values are large as a result of the omission of known exit channels with small transmission coefficients T_{ij} . (For ^{19}F and ^{23}Na targets, all known channels with $T_{ij} \geq 0.05$ were included; for the ^{31}P target, some exit channels to high

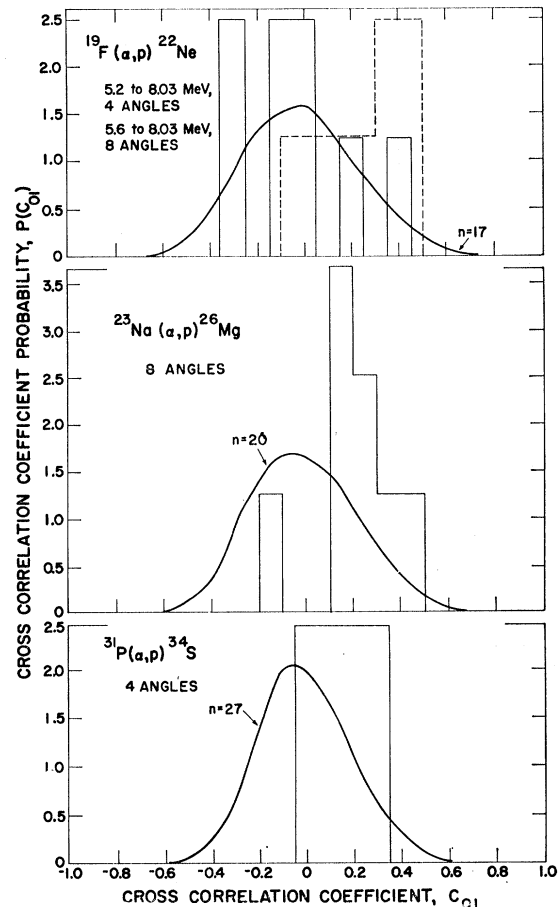


FIG. 20. The frequency distribution function $P(C_{01})$ of the cross correlation C_{01} between data at the same energies ($\epsilon=0$) from the ground- and first-excited-state reactions. Cross correlations were calculated from Eq. (8). The dotted histogram for the ^{19}F case is for the 5.2- to 8.0-MeV range of alpha-particle energy for only the four forward angles. Cross correlations are evident in the 5.2- to 5.6-MeV range. (See Fig. 2.) The curves were obtained from Monte Carlo calculations with $n=17, 20,$ and 27 , respectively, independent χ^2 distributions each with four degrees of freedom ($N=2$).

³³ T. Ericson and V. Strutinski, Nucl. Phys. 8, 284 (1958).

excitation energy were omitted with $T_{ij} \leq 0.3$, but this occurred only for zero orbital angular momentum, $l=0$.)

These calculational difficulties are not expected to affect the $\bar{\sigma}_{\text{CN}}$ values of the ground-state reaction relative to the first-excited-state reaction. Thus the agreement between these relative measured $\langle\sigma_{\text{CN}}\rangle$ values and these relative calculated $\bar{\sigma}_{\text{CN}}$ values for the $^{31}\text{P}(\alpha, p)^{34}\text{S}$ reaction in Fig. 16 is gratifying, especially since this case has the largest sample size. The $^{23}\text{Na}(\alpha, p)^{26}\text{Mg}$ and $^{19}\text{F}(\alpha, p)^{22}\text{Ne}$ cases in Figs. 15 and 14, respectively, have progressively smaller sample sizes and result in progressively less satisfactory agreement between the relative $\langle\sigma_{\text{CN}}\rangle$ values measured for the ground- and first-excited-state reactions and these relative $\bar{\sigma}_{\text{CN}}$ calculated values. Agreement is generally within the large uncertainties, but for the first-excited-state reactions, some evidence of the use of erroneously low $N_{\text{eff}}^{J\pi}$ values exists from the relatively low values of $\langle\sigma_{\text{CN}}\rangle$.

We now consider the direct-reaction cross-section σ_{DI} measurements in Figs. 14 to 16. Here, the forward-peaked angular distribution generally expected for direct reactions is qualitatively obtained. The distorted-wave Born-approximation calculations of σ_{DI} are based on the transfer of a triton, thus the values obtained contain a common factor that results from the uncertainty in the overlap of the proton and triton wave functions with the alpha-particle wave function. A common factor of $\frac{2}{3}$ was applied to these calculated σ_{DI} values for plotting in Figs. 14 to 16 to give agreement with measurements. Again, the $^{31}\text{P}(\alpha, p)^{34}\text{S}$ case with the largest sample size gives best agreement between measurement and calculations. Also, the $^{19}\text{F}(\alpha, p)^{22}\text{Ne}$ case with the smallest sample size gives the poorest agreement; in this case, the back-angle yields are anomalously large. It should be noted that the values of σ_{DI} measured for the ground-state reactions relative to the first-excited-state reactions should not necessarily agree with the relative σ_{DI} values from these calculations. This is because the spectroscopic factors in the calculations were all simply assumed to be unity, but in reality can readily be different for these ground-state reactions and first-excited-state reactions.

For the $^{31}\text{P}(\alpha, p)^{34}\text{S}$ reaction, about twice the incident energy was used as for the other reactions. Thus, it is reasonable that the measured direct-reaction cross section at forward angles is observed to be several times larger than for the ^{19}F and ^{23}Na targets. Nevertheless, the fraction y of direct reactions at forward angles in Fig. 13 is similar for the ^{23}Na and ^{31}P targets. This

is explained by the somewhat small compound-nucleus cross sections $\langle\sigma_{\text{CN}}\rangle$ measured for the ^{19}F and ^{23}Na targets compared to the calculated $\bar{\sigma}_{\text{CN}}$ cross section (see Figs. 14 and 15), while these cross sections for the ^{31}P target are in agreement.

The inverse $^{26}\text{Mg}(p, \alpha)^{23}\text{Na}$ reaction to the $^{23}\text{Na}(\alpha, p)^{26}\text{Mg}$ used here has been studied at higher energies by Allardyce *et al.*⁹ with a sample size n somewhat larger than that of the present measurements. No direct reactions were reported in that analysis.

The same $^{26}\text{Mg}(p, \alpha)^{23}\text{Na}$ inverse reaction has been studied by Lawrence and Hay³⁴ at the same excitation energies we used, but was not analyzed for fluctuations. Their excitation functions, like ours, have no moving average evident in the cross section. For our data, this is seen by the constant averages of the cross sections as a function of energy, examples of which are in Fig. 3. However, this same inverse reaction at higher energies⁹ does clearly show a decrease of the average cross sections with energy. Evidently our excitation functions at our lower compound-nucleus energy are in the flat region of cross section between the Coulomb barrier suppression at lower energies and the suppression by competing exit channels at higher energies. Such effects on the compound-nucleus cross section have clearly been shown¹¹ for heavier nuclei. For our highest energy reaction, $^{31}\text{P}(\alpha, p)^{34}\text{S}$, the excitation functions in Fig. 4 exhibit some small evidence of this moving average effect, but the effect is not apparent as a change in slope in an $N_{\text{eff}}^{\text{exp}}$ analysis of the Gibbs type.⁶ Thus, we do not expect any moving average significantly to affect the cross-section results for this reaction in Fig. 16.

An analysis³⁵ has recently been made of $^{45}\text{Sc}(p, \alpha)^{42}\text{Ca}$ fluctuation data at energies greater than used for our fluorine and sodium targets, but slightly less than for our phosphorus target. The result for back angles was about 60% direct reactions, which agrees with our fluorine and sodium results, but is greater than our phosphorus results.

ACKNOWLEDGMENTS

The authors are grateful to Judith Gursky for preparation of targets, to the operators of the Van de Graaff, and especially to W. R. Gibbs for advice, numerous discussions, and for providing the codes used in the analyses in the paper.

³⁴ L. G. Lawrence and H. J. Hay, Nucl. Phys. 44, 518 (1963).

³⁵ A. Richter, A. Bamberger, P. von Brentano, T. Mayer-Kuckuk, and W. von Witsch, Z. Naturforsch. 21A, No. 7 (1966).